J. Fluid Mech. (2005), *vol.* 543, *pp.* 293–302.
doi:10.1017/S0022112005006713 Printed in the United Kingdom

Axisymmetric gravity currents in a porous medium

By SARAH LYLE[1], HERBERT E. HUPPERT[2], MARK HALLWORTH[2], MIKE BICKLE[1] AND ANDY CHADWICK[3]

[1]Department of Earth Sciences, University of Cambridge, Downing Street, Cambridge CB2 3EQ, UK

[2]Institute of Theoretical Geophysics, Department of Applied Mathematics and Theoretical Physics, University of Cambridge, CMS, Wilberforce Road, Cambridge CB3 0WA, UK

[3]British Geological Survey, Kingsley Dunham Centre, Nottingham NG12 5GG

slyle81@gmail.com, heh1@esc.cam.ac.uk, hallwort@esc.cam.ac.uk, mb72@esc.cam.ac.uk, rach@bgs.ac.uk

(Received 27 June 2005 and in revised form 22 August 2005)

The release from a point source of relatively heavy fluid into a saturated porous medium above an impermeable boundary is considered. A theoretical relationship is compared with experimental data for the rate of propagation of the front of the resulting gravity current and its shape. A motivation of the study, the problem of carbon dioxide sequestration, is briefly discussed.

1. Introduction

Flow in porous media occurs in many natural and industrial situations. Included in these are the seepage of rainwater through permeable ground into an aquifer (EPA 1999), the forced flow of oil from sandstone reservoirs (Lake 1989; Gerritsen & Durlofsky 2005), and the dispersion of polluted liquids through gravel pits (Kreider *et al.* 1999). In some situations the fixed, solid matrix through which the flow passes reacts with the interstitial fluid and the structure and porosity of the matrix change with position and time (Hallworth, Huppert & Woods 2005). Examples of such reactions include the gradual formation of dolomite (Phillips 1991) and the convective flow due to solidification through a mushy layer, which is a region of reactive solid matrix bathed in interstitial fluid (Worster 2000; Aussillous *et al.* 2005).

A gravity current is the flow which occurs whenever fluid intrudes primarily horizontally into fluid of different density. Gravity currents are also observed in many natural and industrial situations. The fundamentals of flows beneath a relatively less dense homogeneous fluid layer at either low (Huppert 1982*a*, *b*, 2000) or high Reynolds number (Benjamin 1968; Hoult 1972) are well known. In recent years additional phenomena due to the effects of rotation (Ungarish & Huppert 1998), and flows over porous media (Acton, Huppert & Worster 2001; Thomas, Marino & Linden 2004), into stratified ambients (Ungarish & Huppert 2002; Maxworthy *et al.* 2002) and over variable topography (Monaghan & Huppert 2005) have been investigated.

An interesting industrial application was recently brought to our attention by the British Geological Survey concerning the forced injection of carbon dioxide at the Sleipner gas field in the North Sea. Carbon dioxide in a supercritical state flows vertically upwards through a porous reservoir rock, due to its buoyancy relative to

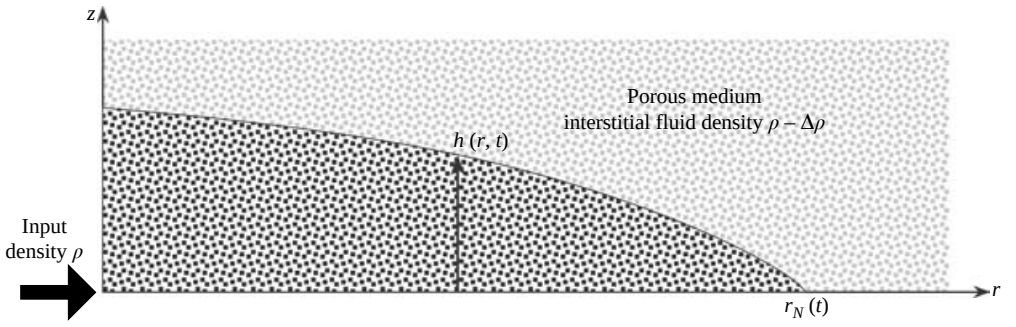

FIGURE 1. A sketch of the gravity current of density ρ and height $h(r, t)$ intruding into a porous medium saturated with fluid of density $\rho - \Delta\rho$.

the surrounding interstitial liquid, and then reaches an impermeable boundary and spreads out below it. This situation is of prime importance to general issues of carbon sequestration. The explicit questions of interest are how rapidly the carbon dioxide spreads, what is the depth of the layer and how do these depend on the physical properties of the carbon dioxide and the solid porous medium through which it is spreading. We plan to present the application of our results in another publication. Here we concentrate on developing standard fluid-mechanical concepts to determine theoretically the rate of evolution of such a gravity current and test the results against laboratory experiments.

There have been numerous investigations of flow in porous media in one dimension, partly because such studies can be experimentally investigated in a Hele-Shaw cell (Huppert & Woods 1995; Woods & Mason 2000). There has also been some work on axisymmetric flow between two closely spaced horizontal plates (Paterson 1981, 1985). In this case the effects of gravity are immaterial and the free surface is confined to the thin, nominally vertical, perimeter of the flow. To the best of our knowledge, this is the first study that investigates experimentally axisymmetric gravity flow in a real porous medium.

In the next section we consider the theoretical development for a relatively heavy current propagating along the horizontal base of an ambient homogeneous porous medium saturated with interstitial fluid of smaller density (under the Boussinesq aproximation this is the equivalent to the natural situation). A conceptually similar problem is described with a quite different form of analysis in Barenblatt, Entow & Ryzhik (1989). Section 3 describes our experimental set-up and discusses how well the experimental data agree with the theoretical predictions. In § 4 we summarize our major new results and conclusions, and compare our results with a related theoretical study by Bachu, Nordbotten & Celia (2005) and Nordbotten, Celia & Bachu (2005).

2. Theoretical development

Consider a Newtonian fluid of uniform density ρ introduced at the base of a permeable medium, saturated with liquid of uniform density $\rho - \Delta\rho$, above a horizontal impermeable boundary as sketched in figure 1. With respect to a horizontal radial coordinate r and a vertical coordinate z, with origin at the source point, the ensuing axisymmetric gravity current has a height $h(r, t)$ and extends to a radius which we denote by $r_N(t)$. (The conditions for axisymmetry are discussed in § 4.) Consider the flux to be such that the total volume of the dense fluid in the porous medium at any

time is given by Qt^{α}, where both Q and α are constant. (A value of $\alpha = 0$ signifies an instantaneous release of a fixed volume Q, while $\alpha = 1$ indicates the release at a constant volume flux, Q. The actual input flux is given by $\alpha Qt^{\alpha-1}$.)

The flow of the current, assumed incompressible, is governed by Darcy's law (Phillips 1991)

$$0 = -\nabla p - \rho \boldsymbol{g} - \frac{\mu}{k}\boldsymbol{u}, \tag{2.1}$$

where p is the pressure, $\boldsymbol{u}$ the velocity of propagation of the current, with horizontal component u, $\boldsymbol{g}$ the gravitational accleration, μ the dynamic viscosity of the intruding fluid and k the permeability of the porous medium, which is assumed to be isotropic. We neglect motion in the fluid saturating the porous medium on the assumption that the thickness of this region greatly exceeds that of the thin current layer, within which the velocity is relatively much larger. Because the motion in the ambient is neglected, its viscosity is immaterial in the calculation. However, the propagating front will be unstable if the viscosity of the intruding fluid is less than that of the fluid already in the porous medium (Couder 1991).

The radial pressure gradient driving the flow is related to the gradient of the unknown free surface by

$$\frac{\partial p}{\partial r} = \rho g' \frac{\partial h}{\partial r}, \tag{2.2}$$

where $g' = g\Delta\rho/\rho$ is the reduced gravity (relative buoyancy), and any capillary forces (surface tension) between the two liquids have been neglected. Introducing (2.2) into the horizontal (radial) component of (2.1), we find that

$$u(r, t) = -(k\rho g'/\mu)\frac{\partial h}{\partial r}. \tag{2.3}$$

The local continuity condition (Huppert 1982*a*; Huppert & Woods 1995) is

$$\phi \frac{\partial h}{\partial t} + \frac{1}{r}\frac{\partial}{\partial r}(ruh) = 0, \tag{2.4}$$

where ϕ is the porosity of the porous medium, which is assumed to be constant in both space and time. Substituting (2.3) into (2.4), we obtain the nonlinear partial differential equation governing the unknown free-surface height $h(r, t)$

$$\frac{\partial h}{\partial t} - \frac{\gamma}{r}\frac{\partial}{\partial r}\left(rh\frac{\partial h}{\partial r}\right) = 0, \tag{2.5}$$

where

$$\gamma = \rho k g'/(\phi\mu). \tag{2.6}$$

To (2.5) must be added the global continuity equation

$$2\pi \int_0^{r_N(t)} rh \, \mathrm{d}r = Qt^{\alpha}, \tag{2.7}$$

along with the boundary condition

$$h[r_N(t), t] = 0. \tag{2.8}$$

This completes the mathematical formulation of the problem.

While it would be relatively easy these days to determine numerical solutions to (2.5) with the added constraints (2.7) and (2.8) for a variety of initial conditions, it is much more insightful to determine similarity solutions, dependent on an appropriate

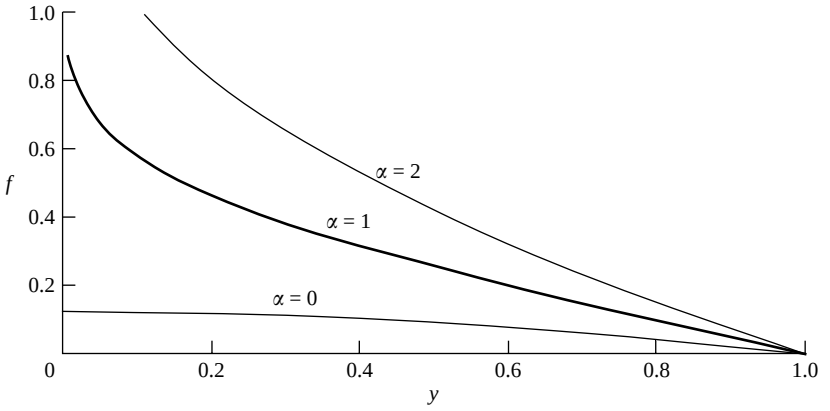

FIGURE 2. Graphs of the shape factor, or eigenfunction f, as a function of the scaled similarity variable y for $\alpha = 0, 1$ and 2.

combination of the independent variables, r and t (Barenblatt 2003). A suitable similarity variable is of the form

$$\eta = (\gamma Q)^{-1/4} r\, t^{-(\alpha+1)/4}, \tag{2.9}$$

from which it follows immediately that the extent of the current is given by

$$r_N(t) = \eta_N(\alpha)(\gamma Q)^{1/4} t^{(\alpha+1)/4}, \tag{2.10}$$

where $\eta_N(\alpha)$ is a function only of α. Equation (2.10) is sufficient to show that a release of a constant volume spreads like $t^{1/4}$, while the response to a constant flux release spreads like $t^{1/2}$.

To evaluate η_N explicitly and the corresponding shape of the current, we introduce

$$h(r,t) = \eta_N^2 (Q/\gamma)^{1/2} t^{(\alpha-1)/2} f[y \equiv \eta(r,t)/\eta(r_N,t], \tag{2.11}$$

where the new independent variable y is a scaled similarity variable which varies between 0 at the source and 1 at the furthest extent of the current. Note that for the important case $\alpha = 1$, considered here in the experiments, $h \propto f$, independent of t (except through η).

Substituting (2.9) and (2.11) into (2.5), we obtain, after quite some algebra,

$$(yff')' + \tfrac{1}{4}(1+\alpha)y^2 f' + \tfrac{1}{2}(1-\alpha)yf = 0, \tag{2.12}$$

$$f(1) = 0, \tag{2.13}$$

$$\eta_N = \left[2\pi \int_0^1 yf(y)\,\mathrm{d}y\right]^{-1/4}. \tag{2.14}$$

For the special, but important case of $\alpha = 0$, (2.12)–(2.14) has solution

$$f(y) = \tfrac{1}{8}(1-y^2) \quad \text{and} \quad \eta_N = 2/\pi^{1/4} \approx 1.502. \tag{2.15}$$

For other values of α, numerical integration is needed. The numerical program was tested by comparing the results with the analytical solution (2.15) and with the limits

$$f = C(-\ln y)^{1/2} \qquad (y \to 0; \alpha > 0), \tag{2.16a}$$

$$f = \tfrac{1}{4}(1+\alpha)(1-y) + 0[(1-\alpha)(1-y)^2] \qquad (y \to 1), \tag{2.16b}$$

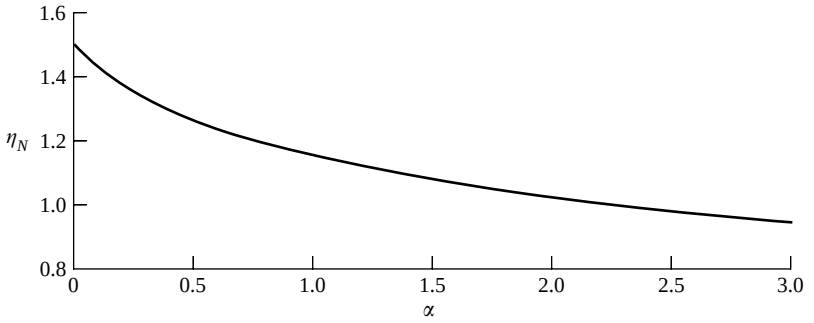

FIGURE 3. The pre-multiplicative constant η_N as a function of α.

where (2.16*a*) is obtained by setting $(yff')' \approx 0$, and (2.16*b*) is the regular perturbation solution of (2.12) and (2.13) in the form $(ff')' + \frac{1}{4}(1+\alpha)f' \approx 0$ and shows that $f = \frac{1}{2}(1-y)[1+0(1-y)^2]$ for $\alpha = 1$.

Figure 2 presents $f(y)$ for $\alpha = 0$, 1 and 2, while figure 3 plots $\eta_N(\alpha)$.

3. Experimental observations

To test the theoretical model we conducted a series of laboratory experiments in which a constant flux ($\alpha = 1$) of a dense salt solution was released from a point source at the base of a porous medium saturated with fresh less dense water. The ensuing gravity current was allowed to spread radially over a solid horizontal boundary. The experiments were performed in a 90° sector tank rather than in a full axisymmetric configuration, because this reduced the volumes of fluid and matrix required for a given radius of tank, and also allowed two vertical profiles of the flow to be observed along perpendicular radial directions. The experimental set-up is shown in figure 4, and consisted of a Perspex tank with a square base of internal side length 61 cm and a depth of 44 cm. The tank was filled to a height of 25 cm with a self-supporting matrix of 3 mm diameter glass ballotini, saturated with fresh water at room temperature. A flexible sheet of Perspex was bent and inserted across two diagonally opposite corners of the tank such that it conformed to a vertical barrier along the circumference of the 90° sector.

At the apex of the sector, a rigid tube of internal diameter 6 mm was positioned vertically in the corner of the tank with its end held 1cm above the solid floor. The tube was linked, via a flexible hose, to a 10 l reservoir containing blue-dyed salt solution suspended 1.7 m above the base of the tank. The gravity-fed flow of salt solution delivered to the tank was controlled by a variable control valve and an additional on/off valve. The volumetric flow rate for any given control valve position was determined by routing the delivery tube into a separate measuring cylinder containing the same height of ballotini matrix as in the experimental tank, designed to mimic the resistance to flow. The overflow collected from delivery into this cylinder over a given time was weighed to determine the flux Q (note that the measured value represents $Q/4$ since we were only measuring the flux to a 90° sector). Once the required flow rate had been established, the flow was temporarily stopped by means of the on/off valve. The delivery tube was then repositioned within the tank and the reservoir was recharged to its initial volume. The flow was re-established to start the experiment, and a blue-dyed gravity current of the dense fluid was observed to spread radially over the base of the tank, with a pore Reynolds number, based on a typical velocity and radius of the ballotini, of the order of 10^{-1}.

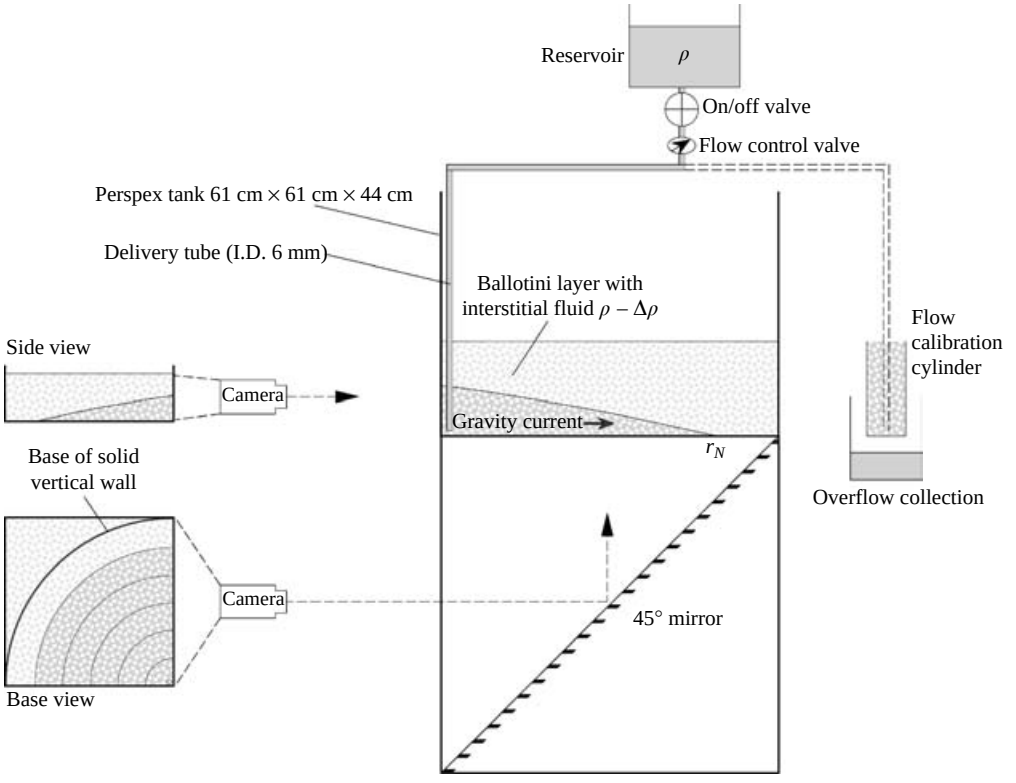

FIGURE 4. A sketch of the experimental set-up showing the two camera positions and how the gravity currents were viewed.

The propagation of the current was measured by directly marking its foremost position to within 1 mm at 5 s time intervals along one of the sidewalls of the tank. In addition, the flow profile was recorded on digital video on the other perpendicular sector wall, along with a sequence of still images of the radial flow across the base of the tank, as observed by means of a 45° mirror positioned under its transparent base. Measurements from these three views were used to confirm the radial symmetry of the current. Once the flow had reached within 5 cm of the confining outer boundary, the flow from the reservoir was stopped and the remaining volume was measured to determine the volume delivered over the known duration of the run. This provided an independent check on the flow rate, and was always found to be in good agreement with the precalibrated value. After each experiment the digital recordings were analysed to yield the flow profile data in terms of height as a function of radius and time.

Nine experiments were performed with various values of the reduced gravity g' and flow rate Q, as presented in table 1. Three of the experiments released the dense salt solution at the top of the layer of ballotini. In figure 5, the radial spread of all the currents, normalized by either $(g'Q)^{1/4}$ or $(\gamma Q)^{1/4}$, as suggested by (2.10), is plotted against time on logarithmic axes, with solid symbols denoting the last three experiments. The data show a very satisfactory collapse, confirming the $t^{1/2}$ power-law relationship predicted by (2.10) and the validity of the scaling by $(g'Q)^{-1/4}$, independent of the position of release of the dense salt solution. The mean value of porosity for these close-packed ballotini is $\phi = 0.37$, from which it follows from either measurement, or use of the Carman–Kozeny relationship, that the mean value of the

Expt	1	2	3	4	5	6	7	8	9
g'(cm s^{-2})	10	20	40	80	40	40	80*	40*	20*
Q(cm^3 s^{-1})	36.8	34.4	34.4	39.2	9.2	72.4	55.0	49.2	72.9
$h_{\max}$(cm) at $r=0$	13.4	11.7	8.9	7.3	5.0	13.4			

TABLE 1. Input values and maximum height at the origin for all experiments including three with input at the top of the ballotini layer (marked * in this table and with a solid symbol in figures 5 and 8).

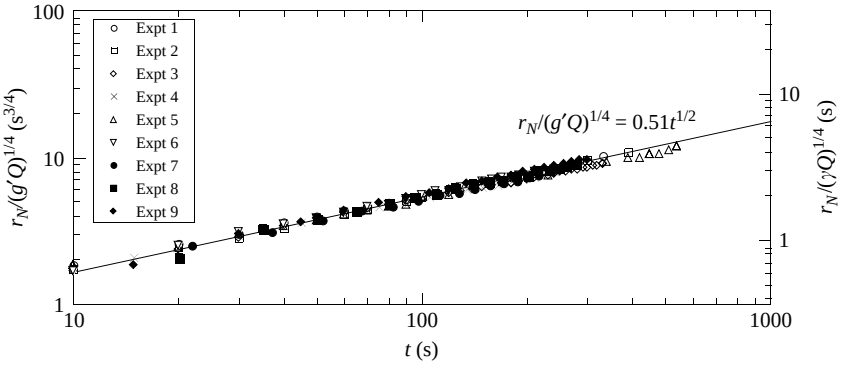

FIGURE 5. The non-dimensionalized radius of propagation, $r_N/(g'Q)^{1/4}$, or $r_N/(\gamma Q)^{1/4}$, as a function of time t on logarithmic axes, for all the experiments, with the values of g' and Q as marked. The best straight-line fit on these logarithmic axes, represents $r_N = 0.51(g'Q)^{1/4}t^{1/2}$.

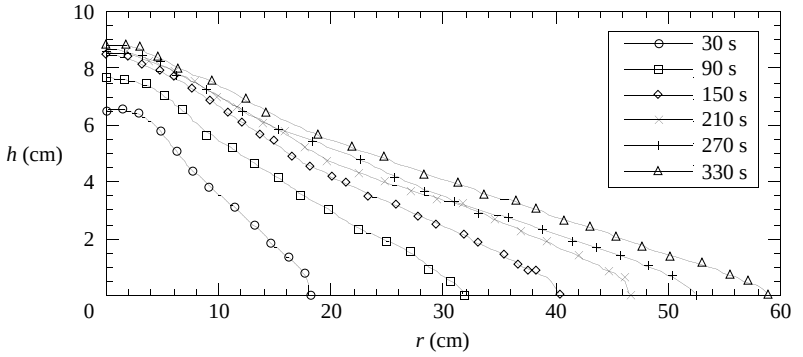

FIGURE 6. The height of the gravity current as a function of r with $g' = 40\,\mathrm{cm\,s^{-2}}$ and $Q = 34.4\,\mathrm{cm^3\,s^{-1}}$ at six different times. The curves have been fit by eye through the data points to illustrate the trend.

permeability is $k = 6.8 \times 10^{-9}\,\mathrm{m^2}$ (Acton *et al.* 2001). Hence $\eta_N(1)(\rho k/\phi\mu)^{1/4} = 0.43$, a value to be compared with the best fit to the experiments, shown in figure 5, of 0.51. The agreement is good, but not excellent, for reasons that will be explained below, after consideration of the experimentally measured profile of the current.

The vertical profiles for a typical experiment are shown in figure 6, which plots the height of a particular current as a function of radius at 60 s intervals. The data for the height of the current for some typical experiments is plotted as a function of the single variable y in figure 7. The satisfactory collapse of these data, at different times and positions, independent of the input position, lends credence to the suitability of the similarity variable $y = \eta(r,t)/\eta(r_N,t)$ suggested in (2.11). The same data normalized

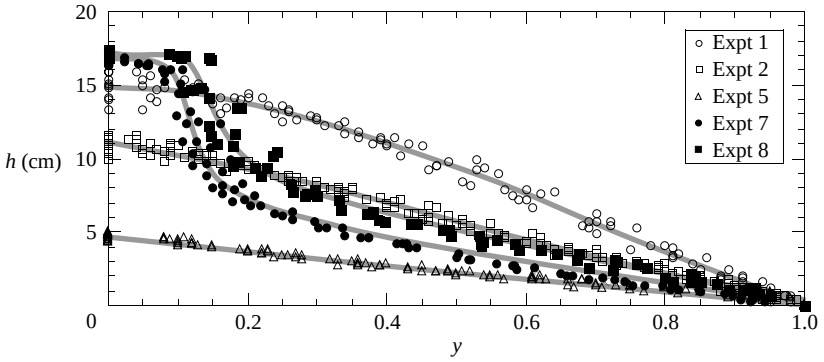

FIGURE 7. Experimental data for the height of five currents as a function of the scaled similarity variable y. The curves through the data points from three experiments with input at the origin (numbers 1, 2 and 5) are the best-fit cubic; the two remaining curves have been drawn by eye.

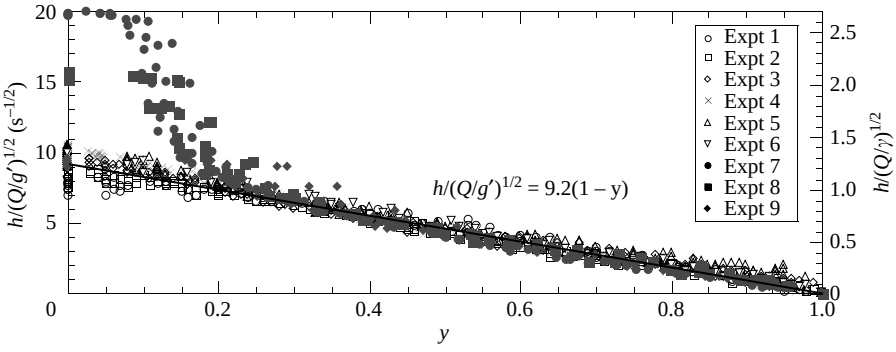

FIGURE 8. The non-dimensionalized height, $h/(Q/g')^{1/2}$ or $h/(Q/\gamma)^{1/2}$ as a function of the scaled non-dimensional variable, y for all the experiments. The best-fit line through the data for $y > 0.2$ indicates that $h = 9.2(1-y)(Q/g')^{1/2}$.

by $(Q/g')^{1/2}$ or $(Q/\gamma)^{1/2}$ are plotted as a function of y in figure 8. The collapse of all the data is confirmation of the appropriateness of the prefactor of $(Q/\gamma)^{1/2}$ suggested by (2.11). The measured functional form is represented well by $h/(Q/g')^{1/2} = 9.2(1-y)$ for $y > 0.2$ (cf. (2.16*a*), which indicates that $f \approx \frac{1}{2}(1-y)$ for $\alpha = 1$ with an error that is of order $(1-y)^2$). However, the measured height differs in detail from the theoretically evaluated curve for $0 < y < 0.2$ shown in figure 2 for $\alpha = 1$ because the input either at the origin of coordinates or at the top of the layer, for the final three runs, does not adequately reflect that taken up by the similarity solution. This could be viewed as an inadequacy of the similarity solution, or, alternatively, as an indication of its robustness: despite the different input employed in the experiments, the similarity solution correctly predicts the form of spread of the front of the current, and does so quantitatively to within a factor of $4.3/5.1 = 0.85$, and also predicts the correct scaling of the gravity current profile in both the vertical and the horizontal.

4. Conclusions and discussion

Our study has shown how a gravity current of either relatively dense or light fluid propagates into a saturated porous medium against a rigid horizontal boundary. By

using similarity variables, we have captured the rate of propagation of the current and the appropriate scaling for its shape. The theoretical model was generally in good agreement with our experimental data. The ideas presented in this first-order simplified model can act as a foundation for further studies investigating other effects. These include the following: a non-horizontal or topographically variable boundary; a non-Newtonian stress–strain law for either the intruding or the intruded fluid, in which case Darcy's Law, as represented by (2.1) will have to be amended; an anisotropic porous matrix, through which, with a significantly smaller vertical than horizontal permeability, the current will spread more rapidly in the horizontal but will confine its expansion in the vertical. Considerable differences in viscosities of the two fluids may exist, but, if the viscosity of the fluid saturating the porous medium is less than that of the current, this should have little effect. However, if the viscosity of the intruding current is the smaller, then an instability akin to the Saffman–Taylor instability (Phillips 1991; Couder 1991) would be expected. We plan to investigate each of these possibilities in future publications.

After the completion of the experiments reported here and the writing of this paper almost finished, our attention was drawn to the interesting recent conference proceedings of Bachu *et al.* (2005) and the follow up (Nordbotten *et al.* 2005). Their purely theoretical study was motivated by the fact that during the last 15 years, oil and gas producers in the Alberta Basin in western Canada have disposed of more than 4.5×10^6 tons of acid gas at 39 locations at rates ranging from 10^3 to 500×10^3 m^3/per day. Nordbotten *et al.* (2005) state explicitly that 'the acid-gas injection operations in western Canada and the United States represent a commercial-scale analog to geological storage of CO_2 which is one of the most promising means of reducing anthroprogenic CO_2 emissions into the atmosphere in the short-to-medium term'. This is indeed a stimulating and important motivation.

Bachu *et al.* (2005) and Nordbotten *et al.* (2005) consider a flux of fluid injected into a layer of vertical height B and allow, in theory, for different viscosities of the fluids (though an axisymmetric analysis must be amended if the viscosity of the intruding fluid is less than that already *in situ*). They write down Darcy's Law, deriving a relationship between the pressure gradient and the free-surface slope of the current, similar in form to (2.2). They then obtain a semi-analytical solution based on energy minimization and variational calculus. The results involve two parameters: one they call a mobility ratio, which is the ratio of the viscosities of the two fluids, while the other bears a similarity to γ defined in (2.6), although it also incorporates B^2 in the numerator. The geometrical set-up of our two studies is different and so no direct comparison is possible. However, it is interesting to note that their suggested radius of the axisymmetric current is proportional to $t^{\alpha/2}$ (equation 10 of Bachu *et al.* (2005) and 6 of Nordbotten *et al.* (2005)) in contrast to $t^{(\alpha+1)/4}$ of (2.10). These agree for $\alpha = 1$, but for no other value of α.

The introduction of the extra length scale, B, invalidates the approach via the method of similarity solutions. Only a full numerical solution will yield reliable results. This might be an interesting project. Until completed, however, the similarity solution presented here will be robust as long as B considerably exceeds $(Q/\gamma)^{1/2}$, the scaled height of the intruding gravity current, even though the excess is only a factor of approximately two for the experiments considered here.

We thank S. Bachu, G. Barenblatt, M. Celia, P. F. Linden, J. Nordbotten, M. Ungarish, A. W. Woods and M. G. Worster for helpful comments on an earlier version of this paper.

REFERENCES

Acton, J. M., Huppert, H. E. & Worster, M. G. 2001 Two-dimensional viscous gravity currents flowing over a deep porous medium. *J. Fluid Mech.* **440**, 359–380.

Aussillous, P., Sederman, A. J., Gladden, A. F., Huppert, H. E. & Worster, M. G. 2005 Magnetic Resonance Imaging of structure and convection in solidifying mushy layers. *J. Fluid Mech.* (submitted).

Bachu, S., Nordbotten, J. M. & Celia, M. A. 2005 Evaluation of the spread of acid-gas plumes injected in deep saline aquifers in Western Canada as an analogue for CO_2 injection into continental sedimentary basins. In *Proc. 7th Intl Conf. Greenhouse Gas Control Technologies*, Volume 1: Peer Review Papers and Plenary Presentations, Vancouver, BC.

Barenblatt, G. I. 2003 *Scaling*. Cambridge University Press.

Barenblatt, G. I., Entov, V. M. & Ryzhik, V. M. 1989 *Theory of Fluid Flows Through Natural Rocks*. Kluwer.

Benjamin, T. B. 1968 Gravity currents and related phenomena. *J. Fluid Mech.* **31**, 209–248.

Couder, Y. 1991 Growth patterns: from the stable curved fronts to fractal structures. In *Chaos, Order and Patterns* (ed. R. Artuso, P. Rvitanovic & G. Cascati). Plenum.

Environmental Protection Agency of the United States 1999 *Ground Water Report to Congress*, available online from www.epa.gov/safewater/gwr/finalgw.pdf.

Gerritsen, M. G. & Durlofsky, L. J. 2005 Modelling fluid flow in oil recovery. *Annu. Rev. Fluid Mech.* **37**, 211–238.

Hallworth, M. A., Huppert, H. E. & Woods, A. W. 2005 Dissolution-driven convection in a reactive porous medium. *J. Fluid Mech.* **535**, 255–285.

Hoult, D. P. 1972 Oil spreading on the sea. *Annu. Rev. Fluid Mech.* **4**, 341–368.

Huppert, H. E. 1982*a* The propagation of two-dimensional and axisymmetric viscous gravity currents over a rigid horizontal surface. *J. Fluid Mech.* **121**, 43–58.

Huppert, H. E. 1982*b* The flow and instability of viscous gravity currents down a slope. *Nature* **300**, 427–429.

Huppert, H. E. 2000 Geological fluid mechanics. In *Perspectives in Fluid Dynamics: A Collective Introduction to Current Research* (ed. G. K. Batchelor, H. K. Moffatt & M. G. Worster), pp. 447–506. Cambridge University Press.

Huppert, H. E. & Woods, A. W. 1995 Gravity-driven flows in porous layers. *J. Fluid Mech.* **292**, 55–69.

Kreider, J. F., Cohen, R. R. H., Cook Jr, N. E. *et al.* 1999 Environmental Engineering. In *Mechanical Engineering Handbook* (ed. F. Kreith). CRC Press.

Lake, L. N. 1989 *Enhanced Oil Recovery*. Prentice-Hall.

Maxworthy, T., Leilich, J., Simpson, J. E. & Meiburg, E. H. 2002 The propagation of a gravity current in a linearly stratified fluid. *J. Fluid Mech.* **453**, 371–394.

Monaghan, J. & Huppert, H. E. 2005 Gravity currents in V-shaped topography. *J. Fluid Mech.* (in preparation).

Nordbotten, J. M., Celia, M. A. & Bachu, S. 2005 Injection and storage of CO_2 in deep saline aquifers: analytic solution for CO_2 plume evolution during injection. *Transp. Porous Med.* **58**, 339–360.

Paterson, L. 1981 Radial fingering in a Hele-Shaw cell. *J. Fluid Mech.* **113**, 513–529.

Paterson, L. 1985 Fingering with miscible fluids in a Hele-Shaw cell. *Phys. Fluids* **28**, 26–30.

Phillips, O. M. 1991 *Flow and Reactions in Permeable Rocks*. Cambridge University Press.

Thomas, L. P., Marino, B. M. & Linden, P. F. 2004 Lock-release inertial gravity currents over a thick porous layer. *J. Fluid Mech.* **503**, 291–319.

Ungarish, M. & Huppert, H. E. 1998 The effects of rotation on axisymmetric, particle-driven gravity currents *J. Fluid Mech.* **362**, 17–51.

Ungarish, M. & Huppert, H. E. 2002 On gravity currents propagating at the base of a stratified ambient. *J. Fluid Mech.* **458**, 283–301.

Woods, A. W. & Mason, R. 2000 The dynamics of two-layer, gravity-driven flows in permeable rock. *J. Fluid Mech.* **421**, 83–114.

Worster, M. G. 2000 Solidification of fluids. In *Perspectives in Fluid Dynamics: A Collective Introduction to Current Research* (ed. G. K. Batchelor, H. K. Moffatt & M. G. Worster), pp. 393–446. Cambridge University Press.